LAWRENCE
LIVERMORE
NATIONAL
LABORATORY

LLNL-JRNL-767293

Influence of light on particulate organic matter utilization by attached and free-living marine bacteria

L. Gomez-Consarnau, D. M. Needham, P. K. Weber, J. A. Fuhrman, X. Mayali

February 4, 2019

Frontiers in Microbiology

Disclaimer

LLNL-JRNL-767293

Influence of light on particulate organic matter utilization by attached and free-living marine bacteria

Laura Gomez-Consarnau[1,2], David M. Needham[1], Peter K. Weber[3], Jed A. Fuhrman[1] and Xavier Mayali[3]

[1]Department of Biological Sciences, University of Southern California, Los Angeles, CA 90089, USA.

[2]Departamento de Oceanografía Biológica, Centro de Investigación Científica y de Educación Superior de Ensenada (CICESE), Ensenada, Baja California 22860, México.

[3]Lawrence Livermore National Laboratory, Livermore CA 94550, USA.

Manuscript length: 6539 words

Abstract

Light plays a central role on primary productivity of aquatic systems. Yet, its potential impact on the degradation of photosynthetically-produced biomass is not well understood. We investigated the patterns of light-induced particle breakdown and bacterial assimilation of detrital C and N using ^{13}C and ^{15}N labeled freeze-thawed diatom cells incubated in laboratory microcosms with a marine microbial community freshly-collected from the Pacific Ocean. Particles incubated in the dark resulted in increased bacterial counts and dissolved organic carbon concentrations compared to those incubated in the light. Light also influenced the attached and

free-living microbial community structure as detected by 16S rRNA gene amplicon sequencing. For example, Sphingobacteriia were enriched on dark-incubated particles and taxa from the family Flavobacteriaceae and the genus *Pseudoalteromonas* were numerically enriched on particles in the light. Isotope incorporation analysis by phylogenetic microarray and NanoSIMS (a method called Chip-SIP) identified free-living and attached microbial taxa able to incorporate N and C from the particles. Some taxa, including members of the Flavobacteriaceae and Cryomorphaceae, exhibited increased isotope incorporation in the light, suggesting the use of photoheterotrophic metabolisms. In contrast, some members of Oceanospirillales and Rhodospirillales showed decreased isotope incorporation in the light, suggesting that their heterotrophic metabolism, particularly when occurring on particles, might increase at night or may be inhibited by sunlight. These results show that light influences particle degradation and C and N incorporation by attached bacteria, suggesting that the transfer between particulate and free-living phases are likely affected by external factors that change with the light regime, such as time of day, water column depth and season.

Introduction

Photoheterotrophy is a major biogeochemical process in surface waters. Although this dogma is now recognized across the aquatic microbiology field (Béjà et al., 2000; Kolber et al., 2000), until the year 2000 all marine heterotrophic bacteria were classified as strict organic matter decomposers. Two major light energy transducing mechanisms are now identified in surface bacterioplankton:

47 proteorhodopsin (PR) photoheterotrophy and aerobic anoxygenic phototrophy
48 (AAP). PRs are the most abundant and widespread of the two. Notably, they are
49 present and highly expressed in many bacteria including those from the SAR11
50 clade (Giovannoni et al., 2005; Gifford et al., 2013; Ottessen et al., 2013, 2014) and
51 most studies suggest that they are ubiquitous in nutrient-depleted waters (e.g. the
52 Eastern Mediterranean Sea; Dubinsky et al., 2017). However, PRs have also been
53 identified in bacteria adapted to grow on organic matter-rich particles such as the
54 Flavobacteriia (Gómez-Consarnau et al., 2007; Gonzalez et al., 2008; Riedel et al.,
55 2013; Maresca et al., 2018). These nutrient-rich particle-associated
56 microenvironments also seem to be preferred by some AAP bacteria, such as the
57 Rhodobacteraceae commonly found after seasonal phytoplankton blooms (e.g.
58 Allers et al., 2007) and during outdoor cultivation of microalgae (Geng et al., 2016).
59 One unanswered question is whether light energy from PR and AAP
60 photoheterotrophy can be used by those microorganisms to optimize their resource
61 utilization for the degradation of complex particulate organic matter.
62
63 Previous studies carried out in free-living communities strongly suggest that
64 photoheterotrophy plays a role in dissolved organic matter (DOM) degradation. A
65 study in the North Pacific subtropical gyre at station ALOHA reported bacterial
66 production rates 48-92% higher in the light compared to the dark using
67 radiolabeled leucine incorporation (Church et al., 2004). While the microbial groups
68 responsible for the observed light-enhanced uptake rates were not identified, the
69 authors attributed this observation to possible *Synechococcus* amino acid uptake.

Similarly, Michelou et al. (2007) showed that light stimulated both amino acid assimilation and bacterial production; in this case the effect did not correlate with cyanobacterial abundances nor with the growth of photoheterotrophic AAP. Other field studies have reported that both *Prochlorococcus* and low nucleic acid (LNA) bacteria (often dominated by the PR-containing SAR11 bacterial clade) show a significant increase in amino acids uptake in the light compared to the dark (Mary et al., 2008; Gómez-Pereira et al., 2013; Evans et al., 2015). These data indicate that photoheterotrophy can help support dissolved organic matter processing. However, whether or not light can also stimulate the uptake or degradation of particulate organic matter is currently unknown.

Although no studies have thus far examined the role of photoheterotrophy in the degradation of algal-derived particles, there is ample literature about the role of particle degradation in ocean carbon cycling (reviewed by Simon et al., 2002). These studies have determined that particle-attached microbes are i) phylogenetically diverse, often (but not always) dominated by Bacteroidetes known to degrade polysaccharides, ii) exhibit high solubilization rates and iii) may release labile substrates into the surrounding water (Azam and Long, 2001). Understanding the interplay between free-living and particle-attached bacteria is key to further constrain the role of particles in elemental cycling. This question has been explored previously in dark incubations of live diatoms in laboratory rolling tanks (Passow et al., 2003), showing initial increases of biomass in particulate aggregates, further suggesting that the attachment of initially free-living bacteria may bring carbon

93 from the free-living to the particulate phase. Bacteria have also been shown to
94 rapidly attach and detach from particles but become irreversibly attached after
95 some period of time (Kiørboe et al., 2003). Particle-attached bacteria exhibit higher
96 bacterial protein production and higher protease activity per cell than when free-
97 living (Grossart et al., 2007). In one example, polysaccharide-degrading bacterial
98 strains could grow on laminarin (one of the most common carbohydrates in the sea)
99 and released glucose and larger glucans in this process (Alderkamp et al., 2007). Yet,
100 no previous reports have documented particulate organic matter (POM) being
101 released and subsequently incorporated by free-living bacteria; furthermore, the
102 role of light and photoheterotrophy in the process of particulate breakdown
103 remains uncharacterized.
104
105 In the current study, we address some of these unanswered questions using
106 laboratory incubations of a microbial community that started as primarily free-
107 living in the presence of stable isotope labeled phytodetrital particles. We aimed to
108 test the hypothesis that photoheterotrophy enhances the transport of organic
109 compounds from particles into bacterial cells, which would be consistent with light
110 promoting the degradation of POM. This process is expected to be more significant
111 in taxa known to be particle-attached photoheterotrophs such as members of
112 Flavobacteria and Rhodobacterales. We carried out laboratory incubation
113 experiments using freshly collected free-living marine bacterial communities with
114 diatom-derived particles to link the activity of both attached and free-living bacteria
115 to the incorporation of particulate material. Dead, isotopically labeled

phytoplankton cells were mixed with marine microbial communities in rolling bottles to increase cell collisions creating larger particles while also keeping them constantly suspended (Shanks & Edmondson 1989). We quantified incorporation of this particulate material by individual bacterial taxa using Chip-SIP, a method that uses stable isotope labeling, hybridization of RNA to phylogenetic microarrays, and isotopic imaging of the arrays using high-resolution secondary ion mass spectrometry (SIMS) with a Cameca NanoSIMS 50 (Mayali et al., 2012).

Materials and Methods

Production of ^{15}N and ^{13}C labeled diatom-derived particles

We used ^{15}N and ^{13}C labeled phytodetrital particles from the diatom *Thalassiossira pseudonana* CCMP 1335 as a representative of phytoplankton-derived organic matter that is likely to reflect the composition of natural particles in the ocean, and dead algal detritus in algal biofuel production ponds. Cultures of the *Thalassiossira pseudonana* CCMP 1335 were grown in *F*/2 medium (Guillard, 1975) with $^{15}NO_3^-$ under continuous light at 20° C. To maximize the incorporation of labeled carbon, bottles containing the medium were tightly shut immediately after autoclaving to prevent equilibration with atmospheric air, and once cooled were bubbled with N_2 gas for 10 minutes to remove $^{12}CO_2$. 99% atm% ^{13}C labeled sodium bicarbonate ($NaH^{13}CO_3$) was added at a concentration of 2 mM. A 100 µL inoculum of *T. pseudonana* already growing in $^{13}CO_2$ and $^{15}NO_3$ medium was added and the cultures

were incubated with the bottle cap shut. After early stationary phase of growth was achieved (approximately two weeks since the beginning of the experiment), cultures were centrifuged at 1200 *g*, the liquid removed, and the pellet washed twice in filtered seawater, and frozen at -80 °C. Pellets were thawed and refrozen four times and washed in filtered artificial seawater to remove DOM from lysed cells, and frozen again before the start of the incubation experiment.

Experimental setup, DOC analyses and bacterial counts. Surface seawater from the Coastal Pacific was collected at the San Pedro Ocean Time Series SPOT Microbial Observatory site (33° 33′N, 118° 24′W) on May 22nd of 2013 and taken to the laboratory within four hours in a temperature-controlled container. The seawater was subsequently gently filtered to remove grazers and 5 μm particles (5 μm pore-size polycarbonate filters, Millipore corp., Billerica, MA), and then distributed into 10 polycarbonate 2-liter cylindrical bottles (Nalgene). SIP-addition treatments were enriched with 0.19 g/L dry weight diatom-derived ^{13}C and ^{15}N labeled particles and incubated in the light (at 150 μmol m^{-2} s^{-1}) or in the dark in triplicate at 18°C in a rolling bottle setup at 0.5 rpm (CellRoll, Inc). Duplicate control treatments with no added particles were incubated in the same temperature-controlled chamber in the light or dark in static bottles. Samples for cell counts, dissolved organic carbon (DOC), DNA and RNA were collected after 72 hours in addition to T_0. While previous studies have shown that incubations of 12 hours are sufficiently long to detect isotope incorporation with Chip-SIP (Mayali et al., 2012), we decided on 72 hours incubations to allow the transfer of particulate C and N to the dissolved phase to

occur. All material used was previously acid washed with 1% HCl and rinsed in double distilled water.

Samples for DOC were collected by filtering 100 ml of sample through 0.2 μm pore-size polycarbonate filters (47 mm, Millipore corp., Billerica, MA). All material in contact for those samples was pre-rinsed with 1M HCl. DOC samples were sent to the Nutrient Analysis Lab at University of Maryland for analysis. Samples for bacterial counts were preserved in 10% formalin and kept at 4˚C until processing. Two milliliters of the formalin-fixed samples were stained using acridine orange (Hobbie et al., 1977), filtered onto 0.2 μm pore-size black polycarbonate Track-Etched (PCTE) filters (25 mm, Fisher Scientific) and counted with epifluorescence microscopy. Samples for DNA and RNA were collected on 5 μm pore size polycarbonate filters (47 mm, Millipore corp., Billerica, MA), representing large particles, henceforth referred to as "particulate", and the filtrate sequentially collected on 0.2 μm pore size filters (47 mm diameter Durapore® Membrane Filters, Millipore corp. Billerica, MA), representing free-living microbes and those attached to small particles, henceforth referred to as "free-living".

Nucleic acid extraction, and sequencing RNA and DNA from particles (> 5 μm) and free-living bacteria (0.2-5 μm) from all replicates was extracted with the Qiagen AllPrep kit according to manufacturer's instructions for bacterial nucleic acid, using 10 mg/mL lysozyme in the lysis step and including vortexing for 10 min. Microbial diversity in the different treatments and size fractions was assessed by amplifying the V4 and V5 region of the 16S rRNA gene from the DNA extracts using primers

515F and 926R, and paired end 2x300 sequencing on MiSeq (Illumina; Parada et al., 2015). In addition to bacterial and archaeal 16S rRNA gene sequences, these primers also amplify chloroplastic 16S rRNA gene sequences and eukaryotic 18S rRNA gene sequences (Parada et al., 2015; Needham and Fuhrman, 2016), allowing determination of the relative ratios of rRNA genes within the domains Bacteria and Archaea to those of Eukarya. Demultiplexed sequences were quality filtered with Trimmomatic (Bolger et al., 2014), trimming reads with the following settings: SLIDINGWINDOW:5:30, MINLEN:250. Paired end reads were then merged with usearch fastq_mergepairs with the following settings: -fastq_truncqual 5 -fastq_maxdiffs 0 -fastq_minmergelen 200 -fastq_minovlen 50 (Edgar, 2010). Only 16S rRNA gene sequences will be merged at this step, as the 18S rRNA amplicons in this region are about 200 bp longer and as such do not overlap (see below). For merged sequences, primer sequences were removed with cutadapt (Martin, 2011). Chimeric sequences were identified in QIIME (Caporaso et al., 2010) with identify_chimeric_seqs.py using a de novo and referenced based approach using the usearch61 method and the SILVA GOLD database (Quast et al., 2013). Operational taxonomical units (OTU) were determined using the uclust in QIIME with 99% similarity cutoffs. The most abundant sequence within each OTU was selected as a representative sequence. Each representative sequence was assigned classification with QIIME assign_taxonomy.py against the SILVA 111 database via the uclust algorithm. OTUs classified as chloroplastic at this step were then further classified with Phytoref.

After processing of the overlapped reads for 16S rRNA analyses, in order to assess the number of eukaryotic reads in our dataset, we searched all individual paired reads against separate 18S and 16S rRNA gene database from SILVA and selected the paired reads with a higher percent similarity to the 18S dataset compared to the 16S via bbsplit.sh (https://github.com/jcmcnch/eASV-pipeline-for-515Y-926R). Then the sequences were concatenated with an N separating the two reads and OTUs were generated as previously described (Needham and Fuhrman 2016). The OTUs were classified in QIIME via the RDP classifier (Wang et al., 2007) against the PR2 database (Guillou et al., 2013).

For identification of bacterial and archaeal 16S rRNA gene sequence OTUs that were significantly more or less abundant in the different treatments and controls, we used the software packages phyloseq (McMurdie and Holmes, 2013) and DESeq2 (Love et al., 2014). Biom tables of read counts produced from the QIIME pipeline were imported into R via *import_biom* of the phyloseq package. For samples where technical replicates were available (n=2), the reads from the replicates were summed. Then, the phyloseq object was converted to deseq2 objects via *phyloseq_to_deseq2* for each statistical comparison of interest (light *vs*. dark, large *vs.* small, and control *vs*. experimental treatment). For determination of differential abundance between the experimental treatments (i.e., light *vs.* dark, and large *vs*. small size fraction), all of the different treatments of the other factor were used (that is, for example, data from both size fractions were used to determine significant shifts in light vs dark treatments). Significant differences were determined with the

DESeq command using a "Wald" test and a "parametric" fitType (i.e., the default settings). Results were converted to a results table with the DESeq *results* command, retaining all results for further exploration (i.e., cooksCutoff=F). Significant shifts were identified as those with a Benjamini-Hochberg adjusted p-value < 0.05. Heatmaps were generated with the program “heatmap3” in R. Phylogenetic trees were generated by alignment with MUSCLE (-maxiters 100; Edgar, 2004) and maximum likelihood tree generation with phyml (Guindon et al., 2010). Those included amplicon representative sequences from the experimental taxa, together with relevant environmental sequences of previously reported phytoplankton bloom responders at SPOT (Needham and Fuhrman, 2016; Needham et al., 2018) and whole genome sequenced bacteria.

Probe design. We aimed to target organisms commonly found at SPOT as well as those that become enriched on diatom-derived particles. For the former, sequences collected at SPOT were obtained from published literature (Brown et al., 2005; Needham et al., 2013). For the latter, we used probes from a previous Chip-SIP study that targeted dead *T. pseudonana* particle attached bacteria (Mayali et al., 2016). For probes targeting both diatom detritus and SPOT sequences, trimmed sequences were manually checked for quality and submitted to DECIPHER's Find Chimeras web tool (Wright et al., 2012), aligned with the online SINA aligner (Pruesse et al., 2007) and imported into SILVA database SSU_NR ver. 103 in the ARB software (Ludwig et al., 2004), which included 263,000 small subunit ribosomal RNA sequences. Sequences were added to the global phylogeny and 148 unique

253 operational taxonomic units (OTUs) were identified. For each OTU, a set of 25
254 probes targeting the OTU and closely related sequences were designed (Table S1)
255 using the probe design function in ARB. In most cases, probes were allowed to
256 perfectly match with less than 5 sequences outside the targeted group (preferably
257 none, but this was not always possible). Also, in most cases we required that two
258 base-pair changes on the probe sequence (i.e., mismatches) did not match more
259 than 100 sequences outside the targeted group. Our approach was to have multiple
260 probes for each taxon, including probes that target the same region but are offset by
261 a few bases in either direction. This leads to a range of probe melting temperatures
262 for each taxon, and decreases the likelihood that a single probe exhibits non-specific
263 signal. The isotope enrichment of taxa was subsequently compared among one
264 another in relation to the probe hybridization strength, as further explained below.
265
266 **Chip-SIP analyses** RNA samples were split: one fraction saved for fluorescent
267 labeling, the other was unlabeled for NanoSIMS analysis. Fluorescent Alexafluor 532
268 labeling was carried out with the Ulysis kit (Invitrogen) for 10 min at 90°C (2 μL
269 RNA, 10 μL labeling buffer, 2 μL Alexafluor reagent), followed by fragmentation. All
270 RNA (fluorescently labeled or not) was fragmented using 1X fragmentation buffer
271 (Affymetrix) for 10 min at 90°C before hybridization and concentrated by
272 isopropanol precipitation to a final concentration of 500 ng μL^{-1}. Glass slides coated
273 with indium-tin oxide (ITO; Sigma) were coated with silane Super Epoxy 2 (Arrayit
274 Corporation) to provide a starting matrix for DNA synthesis. Custom-designed

275 microarrays (spot size = 17 μm) were synthesized using a photolabile deprotection
276 strategy (Singh-Gasson et al., 1999) by Roche Nimblegen (Roche Nimblegen,
277 Madison, WI). Reagents for synthesis (Roche Nimblegen) were delivered through
278 the Expedite (PerSeptive Biosystems) system. For array hybridization, RNA samples
279 (1 μg) in 1X Hybridization buffer (Roche Nimblegen) were placed in Nimblegen X12
280 mixer slides and incubated inside a Maui hybridization system (BioMicro®
281 Systems) for 18 hrs at 42 °C and subsequently washed according to manufacturer's
282 instructions (Roche Nimblegen). Arrays with fluorescently labeled RNA were
283 imaged with a Genepix 4000B fluorescence scanner at pmt = 650 units. Secondary
284 ion mass spectrometry analysis of microarrays hybridized with rRNA from the ^{13}C-
285 and ^{15}N-labeled particle incubations was performed at LLNL with a Cameca
286 NanoSIMS 50 (Cameca, Gennevilliers, France). A Cs+ primary ion beam was used to
287 enhance the generation of negative secondary ions. Carbon isotopic ratios were
288 determined on electron multipliers in pulse counting mode, measuring $^{12}C^{14}N^-$ and
289 $^{12}C^{15}N^-$ simultaneously, and then $^{12}C^{14}N^-$ and $^{13}C^{14}N^-$ simultaneously. More details of
290 the instrument parameters are provided elsewhere (Mayali et al., 2012). Ion images
291 were stitched together, processed to generate isotopic ratios, and regions of
292 interests (ROIs) of the individual probe spots extracted with the L'IMAGE software
293 (L. Nittler, Carnegie Institution of Washington). Data were corrected for the
294 background isotope ratios measured on probe spots hybridized with control
295 oligonucleotides. For fluorescence, triplicate samples were combined and
296 hybridized on the same microarray (4 total samples: FL dark, FL light, AT dark, AT
297 light). For NanoSIMS, all replicates were analyzed separately (12 total samples). We

298 determined what OTUs in the different treatments were statistically isotopically
299 enriched as described below. For each OTU and for each replicate of all treatments,
300 ^{15}N enrichment (in permil) of individual probe spots was plotted versus
301 fluorescence and a linear regression slope, which we refer to as the hybridization-
302 corrected enrichment (HCE), was calculated. We carried out this calculation with the
303 ^{15}N data as the ^{13}C exhibits higher background and thus lower signal to noise. OTUs
304 were considered significantly isotopically enriched if the slope minus two calculated
305 standard errors (SE) was greater than zero and if the slope was significant based on
306 a t-score statistic (t = slope/SE) with a p-value of less than 0.05 adjusted with the
307 Benjamini-Hochberg false discovery rate procedure. We considered an OTU
308 enriched in a particular treatment if two out of three replicates were statistically
309 significantly enriched.

310

311 The second type of analysis tested differential isotope labeling of the same probes
312 with an analysis of covariance (ANCOVA) using the software JMP v.8.0 (Statistical
313 Discovery™). This method applies a standard least squares approach to determine
314 if the treatment significantly affected the slope of enrichment over fluorescence. We
315 tested the effect of light, both on free-living and attached fractions, as well as the
316 effect of attachment, both on light and dark incubated samples, on the HCE slope.
317 The treatment effect (either light *vs.* dark or particle *vs.* free-living) was used as
318 "independent effect" or "interaction effect" on the relationship between
319 fluorescence and isotope enrichment. In these analyses, the model tested the
320 contributions of three components on the isotope enrichment: 1) the experimental

treatment (e.g. light vs. dark or attached vs. free-living), 2) the fluorescence, and 3) the interaction of treatment and fluorescence, so called the crossed effect. We used this latter component (the interaction effect) as an indication of the treatment having a significant effect on the isotope incorporation.

Results

Microbial community response to particles

Following the 72-hour incubation of Pacific Ocean microbial cells in the presence of phytodetrital particles, both cell and DOC concentrations increased compared to the control (no particle) incubations (Fig. 1). Cell and DOC concentrations were positively correlated with one another for both control ($r=0.95$, $p=0.05$) and particle ($r=0.83$, $p=0.04$) incubations, suggesting that higher DOC concentrations supported increased microbial growth and vice versa. Furthermore, the dark particle incubations exhibited significantly higher cell abundances (15% increase, $p=0.006$) and DOC concentrations (65% increase, $p=0.01$) compared to the light incubations. The particles remained visibly larger and greener after incubation in the dark (Fig. S1), suggesting light-enhanced chlorophyll degradation occurred in the light treatment, as previously observed (Rontani et al., 2001; Mayer et al., 2009).

A total of 348,385 high-quality, merged 16S rRNA reads were obtained from 15 samples. After removal of chimeras (1.2% of sequences) and singletons, we

obtained 1,262 OTUs clustered at 99%, including 592 that were detected in the particle-addition treatments. The majority of sequences were classified into the domains Bacteria or Archaea (99.23-99.80%), while 0.05-0.99% were eukaryotic or belonged to chloroplasts (Table S2). Microbial communities in all incubations were dominated by Gammaproteobacteria (Fig. 2), and this was more pronounced in the particle-attached fraction (>80% OTUs) compared to the free-living (~65%). The clearest patterns of differential abundance were OTUs numerically enriched in the particle treatments compared to the controls (which were numerically dominated by SAR11 OTUs; Figs. 2, S2). The particle enrichment treatments experienced a clear shift in community composition (Figs. 2, 3) with increased numbers of OTUs belonging to Flavobacteriales, Rhodobacterales, Alteromonadales, and Vibrionales (Figs. 2, S2). In general, these taxa are known copiotrophs (Buchan et al., 2014) commonly found to be associated with naturally-occurring particles in marine samples, thus we focus the rest of our analyses on the specific taxa with distinct distribution patterns within the particle addition treatments.

Several differences between the free-living *vs.* particle-attached fractions were identified (Fig. 2). Within the Gammaproteobacteria, Pseudoalteromonadaceae OTUs were in significantly higher relative abundances attached to particles compared to free-living, and also higher in the light compared to the dark. Conversely, Colwelliaceae and Vibrionales abundances increased in the free-living fractions compared to the attached fraction. Bacteroidetes were the second most abundant group detected in our samples. In contrast to many of the

366 Gammaproteobacteria, the relative abundance of Bacteroidetes was twice as high in
367 the free-living fractions (~30%) compared to the particle attached fractions
368 (~15%). Within Bacteroidetes, >95% of the OTUs belonged to Flavobacteriia, with
369 5% of the reads belonging to Sphingobacteriia that were found exclusively in the
370 dark particle-attached treatment (Fig. 2). Alphaproteobacteria and Cyanobacteria
371 were the taxa with the overall lowest abundances in the particle addition treatments
372 (Fig. 2). Alphaproteobacteria OTU abundances were higher in the dark treatments,
373 Rhodobacterales being the most abundant, especially in the particle-attached
374 treatments (>75% of all Alphaproteobacteria) compared to the free-living (50-
375 60%). Also within Alphaproteobacteria, the Rickettsiales were most abundant in the
376 free-living fractions of both light and dark incubations. Cyanobacteria were detected
377 only in the light free-living samples.

378

379 The patterns described above at higher taxonomic levels were mainly driven by the
380 appearance of individual OTUs from those taxa in the particle incubations. Many
381 OTUs significantly responded to light regime, particle attachment, or both (adjusted
382 $p < 0.05$, Fig. 3). A total of 6 OTUs were numerically enriched in the light treatments,
383 including 3 Flavobacteriales and 2 Alteromonadales. We also identified 12 OTUs
384 numerically enriched in the dark treatments, including 6 Flavobacteriales and 2
385 Rhodobacterales. Within the particle incubations, 32 OTUs were numerically
386 enriched in the large particle fractions (> 5 μm), including 12 Gammaproteobacteria
387 and 8 Flavobacteria. Twenty-one OTUs were numerically enriched in the smaller
388 size fraction (5 to 0.22 μm), including 2 SAR11, 10 Gammaproteobacteria, and 5

Flavobacteria. Of the above mentioned OTUs, only two were significantly enriched in specific combinations of light regime and particle attachment: one Rhodobacterales (Marivita sp.) and one Pseudoalteromonas OTU, both as particle attached in the dark (Fig. 3).

Incorporation of isotope labeled particulate organic matter

Out of a total of 156 OTUs targeted by the microarrays, 53 OTUs were not isotopically enriched in any of the 12 samples, and another 7 were not enriched in at least two replicates of the same treatment (Fig. S3). This is a common phenomenon documented in previous Chip-SIP studies (Mayali et al., 2012) as well as density gradient SIP (Dumont and Murrell, 2005). These unenriched taxa represent organisms that were either i) in extremely low abundance in the samples or not present at all, ii) present in the sampled seawater but not growing in the bottled incubations, or iii) growing but did not incorporate C and N derived from the particles. We focus our subsequent data analyses and discussions on taxa that significantly incorporated labeled C and N from the particles. Most OTUs significantly enriched based on our criteria were, indeed, labeled in all treatments and size fractions (i.e. attached, free-living, light, dark). This shows that within the 72-hour incubation, particulate C and N was incorporated by both attached and free-living bacteria, and that this occurred both in the dark and in the light.

To obtain a taxonomic breakdown of particle-derived isotope incorporation from the different incubations and size fractions, we took the HCE values (corresponding to relative isotope incorporation) for each OTU for all replicates and averaged those values across the most abundant bacterial families. This calculation represents the relative isotope incorporation for each family, but does not take into account the abundances of those families in the samples. In order to estimate their total contribution to particulate N incorporation, we multiplied the relative isotope incorporation for each family by the percentage of reads corresponding to that family found in each of the treatments and size fractions. These calculated values should approximate the amount of isotope assimilated by the respective families in the four sample types (Fig. 4), if we assume that 16S rRNA gene read abundances correspond to relative abundances in the samples. The patterns of stable isotope incorporation in the different treatments were similar to those observed in the overall microbial community structure, retrieved by 16S iTAG sequencing. We found that the families Alteromonadaceae, Flavobacteriaceae, and Colwelliaceae dominated the isotope incorporation in the two experimental treatments with added particles. In the attached fractions, the Alteromonadaceae was particularly dominant, responsible for greater than 50% of the incorporation, both in the dark and light treatment. On the other hand, in the free-living fractions, the Flavobacteriaceae dominated isotope incorporation (48% in the dark incubations and 43% in the light; Fig. 4). As also observed by iTAG sequencing, the family Colwelliaceae incorporated the isotope mostly in the free-living fractions (24-27%) compared to the particle attached (9-16%). Other less abundant families

contributed less than 1% of the isotope incorporation, with the exception of Rhodospirillaceae (5%) and Rhodobacteriaceae (3%) in the attached fraction of the dark treatment.

Influence of light on isotope incorporation

Using covariance analysis (ANCOVA, Fig. S4), we tested which OTUs exhibited significantly distinct isotope labeling patterns according to treatment (light *vs*. dark) and size fraction (free-living *vs.* attached; Table 1). These represent taxa with significant treatment and fluorescence crossed effects on isotope labeling, with adjusted p-values <0.05. We identified 6 particle-attached OTUs that incorporated significantly more isotope in the light compared to the dark. These OTUs represented some of the most abundant taxa found in the samples according to the 16S rRNA gene sequencing data, and included the genera *Pseudoalteromonas*, *Colwellia*, and members of the Flavobacteriaceae family. One of the Flavobacteriaceae OTU (Owenweeksia) was the only OTU that also exhibited increased incorporation in the light-incubated free-living samples compared to the dark-incubated samples. Seven other OTUs exhibited the opposite pattern when attached to particles, with significantly higher isotope incorporation in the dark. These included less abundant taxa, such as OTUs from the Oceanospirillales, Rhodospirillales, uncultured Flavobactericeae, uncultured Legionellaceae, and the Sva0996 marine group from the Actinobacteria. The remaining OTUs showing differential isotope incorporation were exclusively more enriched in the free-living

455 compared to the particle attached phase (Table 1). Some of these taxa exhibited
456 differential labeling patterns both in the light and in the dark, or in one but not the
457 other treatment.

458

459 **Discussion**

460 Our experimental setup was designed to use a taxon-specific, isotope labeling
461 method (Chip-SIP) to quantify C and N incorporation by bacteria colonizing
462 phytodetrital particles in laboratory incubations. We used freeze-thawed diatoms as
463 model phytodetrital particles, an approach carried out in a number of previous
464 studies (Bidle & Azam, 1999; Ploug, 2001), as they mimic natural sources of
465 particulate C and N, which are degraded by microbial communities as they sink in
466 the ocean. These types of studies are also valuable to understand the fate of algal
467 detritus in outdoor raceway ponds used for biofuel production (Milledge & Heaven
468 2013). To our knowledge, this is the first such study to utilize stable isotope labeling
469 of the particulate algal material to trace its fate through the community. We added
470 the impact of light in our experimental design to further examine how
471 photoheterotrophic processes affect C and N cycling as bacteria colonized the
472 particles. Different OTUs responded to all possible combinations of particle
473 attachment vs free-living lifestyle under light or dark conditions, at the level of 16S
474 rRNA gene relative abundances. We further observed that some of these taxa
475 showed differential labeling patterns, some in the light and others in the dark, as
476 well as differential labeling between free-living and attached. The most common

pattern was higher isotope incorporation in the free-living phase compared to attached (Table 1). This finding was initially rather puzzling since the isotope labeling originated from the particles and we expected isotope incorporation to be greater when the bacteria were particle-attached. However, previous work has shown that particle-attached bacteria exhibit greater per-cell enzyme activities but slower growth compared to their free-living counterparts, in other words, a decoupling between enzyme hydrolysis and uptake (Beier and Bertilsson, 2011, Unanue et al., 1998). Furthermore, some of the taxa responsible for the first stages of particles degradation might have later been transferred to the small fraction after 72 hours, as we discuss below.

Bacterial dynamics of phytodetrital particle degradation

Bacterial growth dynamics that follow algal blooms involve sequential steps of particle breakdown that are performed by different members of the microbial community. Consistent with our findings of Alteromomadaceae playing a major role in particle degradation, Sarmeto and Gasol (2012) found that *Alteromonas* dominated the uptake of radiolabeled diatom particles during 24-hour incubations. However, the first taxa to colonize phytodetrital particles after 5 hours were members of the Flavobacteria. Several other studies also identified Flavobacteria as the first and major taxa consuming algal bloom biomass (Williams et al., 2013; Kirchman 2002; Gomez-Pereira et al., 2012). The length of our incubations (72 hours) did not allow observing the taxa that initially attached to the diatom

499 particles. Even though previous studies have shown that incubations of 12 hours are
500 sufficiently long to detect isotope incorporation with Chip-SIP (Mayali et al., 2012),
501 we decided on extended incubations of three days to allow the transfer of
502 particulate C and N to the dissolved phase to occur. Therefore, it is possible that
503 members of the Flavobacteria may have been, indeed, the first taxa to respond in
504 our incubations. These initial steps would involve attaching to the particles, starting
505 to degrade complex organic matter using exoenzymes (Kirchman, 2002; Teeling et
506 al., 2012) and releasing smaller breakdown products. After this first response,
507 during which large particles are beginning to be broken down, Flavobacteria
508 increase their relative abundances in the small fraction while the Alteromonadales
509 dominate on particles, potentially taking advantage of less complex organic
510 molecules produced by the Flavobacteria. We further hypothesize that this process
511 may have been more efficient in the light due to proteorhodopsin
512 photoheterotrophy. This would be consistent with the high relative abundance of
513 flavobacterial rhodopsin genes and transcripts found in particle-associated natural
514 samples from surface waters (Maresca et al., 2018). Additionally, Flavobacteria
515 TonB transporters rely on proton gradients and have been shown to be highly
516 expressed during the peak of algal blooms (Teeling et al., 2012), suggesting a role of
517 PR electrochemical gradients in these transport processes (Gómez-Consarnau et al.,
518 2016). It therefore seems plausible that, in the marine environment, the first stages
519 of diatom biomass degradation would generally be carried out mostly by
520 photoheterotrophic Flavobacteria still within the photic zone, and that the
521 subsequent stages of organic matter degradation would take place regardless of

light as particles sink below the photic zone. Overall, there are numerous cooperative processes among members of the microbial community to accomplish the ultimate degradation of phytodetrital material, as suggested for other microbial processes in the ocean (Morris et al., 2012). Future research tracking down the transfer of biomass at different stages of an algal bloom will be necessary to better identify the role of photoheterotrophy in these first steps of algal biomass degradation.

Light-induced microbial community response to organic particles

One of the goals of this study was to identify microbial taxa able to occupy different niches as consumers of marine organic matter in the photic zone. These include i) particle-attached phototrophs, which would take advantage of light through photoheterotrophy to enhance the transport and uptake of complex particulate organic matter, ii) particle-attached chemoheterotrophs, which include decomposers of labile complex organic matter in particles without using light, iii) free-living phototrophs, which are bacterial groups potentially specialized in the light-mediated utilization of smaller organic molecules that remain in seawater after being released from different sources (e.g. particle dissolution, viral lysis) and iv) free-living chemoheterotrophs, which solely rely on dissolved organic matter utilization without using light. Using our experimental incubation approach and examining relative abundance of the 16S rRNA gene and isotope incorporation differences between treatments, we were able to identify several patterns of niche

preference at various taxonomic levels, including some that were only detected at the OTU level.

Particle-attached chemoheterotrophs vs. particle-attached photoheterotrophs. Taxa in the family Alteromonadaceae clearly dominated the phytodetrital particle incubations, with some OTUs with higher relative abundances in the attached microbial fraction and others in the free-living. Light regime, however, did not have an effect on their overall abundances (except for two OTUs with greater abundances in the light treatment). Isotope incorporation for several OTUs from this family, however, was greater in the light compared to the dark (Table 2). Alteromonadaceae are known for their opportunistic lifestyles and great capacity for growing on pulses of organic matter (Allers et al., 2007). There are virtually no phototrophs known in this family (Pinhassi et al., 2016), which would explain the general lack of growth response to light regime in our incubation experiments. Increased isotope incorporation in the light (Table 1), however, could have been a result of i) photolysis of the photodetrytal particles (Mayer et al., 2009) or ii) other microbial taxa using photoheterotrophy to start degrading high molecular weight compounds. These two processes could potentially increase the availability of newly produced low molecular DOM for the Alteromonadaceae. Thus, our data are consistent with the idea that a light-mediated process can lead to an increased C and N transfer to non-phototrophic bacteria.

A number of other OTUs, including members of the orders Oceanospirillales, Rhodospirillales, and other Flavobacteriales, on the other hand, incorporated relatively more isotope and some of them were more abundant in the particle-attached dark treatment compared to the light. These taxa may be inhibited by light or the combination of light and organic matter availability, which can cause the formation of reactive oxygen species. While light wavelengths within the visible spectrum range have been shown to stimulate the overall bacterial activity at the community level, certain bacterial groups may experience light inhibition (reviewed by Ruiz-Gonzalez et al., 2013). Interestingly, the majority of the taxa with higher isotope incorporation in the dark correspond to sequences originally sampled from the deepest SPOT station (890 m depth; Table 1), consistent with the notion that these taxa are better adapted to dark conditions.

One surprising result from the isotope incorporation and the relative abundance data was the lack of an effect of light on the family Rhodobacteriaceae. Many of these taxa are aerobic anoxygenic phototrophs, using bacteriochlorophyll to harvest light energy (Koblížek, 2105). While several studies show that light seldom stimulates their growth and overall cell numbers (e.g. Ferrera et al., 2011), it can increase their substrate uptake rates (Ferrera et al., 2017). Rhodobacteriaceae are also known to increase in abundance during phytoplankton blooms, presumably consuming freshly synthesized organic matter and often associated with particles (Buchan et al., 2014; Teeling et al., 2016). It is possible that due to our experimental setup consisting of 24-hour continuous light incubations, photoheterotrophic metabolism

588 by AAP bacteria may have been inhibited in the light, as bacteriochlorophyll is
589 synthesized during the dark cycle (Wagner-Döbler and Biebl, 2006).

590

591 *Free –living chemoheterotrophs vs. free-living photoheterotrophs.* A number of
592 studies have now shown that free-living strict chemoheterotrophy is not the most
593 successful metabolism in surface waters, as the majority of bacteria in these
594 environments are known free-living photoheterotrophs containing genes for
595 proteorhodopsin phototrophy (80-100% of picoplankton genomes) or aerobic
596 anoxygenic photosynthesis (5-30% of genomes; Dubinsky et al., 2017; Brindefalk et
597 al., 2016; Sieradzki et al., 2018). In this study, we identified several free-living OTUs
598 that became numerically enriched in the light compared to the dark, and one that
599 exhibited increased relative isotope incorporation in the light versus the dark. These
600 included several Flavobacteria OTUs, a family with numerous representatives
601 containing PR genes (e.g. Yoshizawa et al., 2014; Gómez-Consarnau et al., 2007;
602 Gonzalez et al., 2008; Inoue et al., 2013). However, some other Flavobacteria OTUs
603 were enriched in the dark treatments instead, suggesting a chemoheterotrophic
604 lifestyle by those organisms. Indeed, not all marine Flavobacteria strains in culture
605 contain PR genes in their genomes (Fernandez-Gomez et al., 2013), and even the
606 ones that do seem to only respond to light when organic matter is scarce and
607 additional scavenging capacities are needed (Gómez-Consarnau et al., 2007, 2016).
608 A key factor in this light-induced response is that the threshold at which a
609 population experiences substrate limitation – by type of molecule and
610 concentration– can be different from strain to strain (Hagström et al., 2017). Still, as

611 discussed above, photoheterotrophic members of Flavobacteria may have been
612 important in the first particle degradation steps of our light incubations. Our
613 present experimental data cannot confirm this and future research will be needed to
614 better understand their role on particle degradation. Nevertheless, our observations
615 reflect a high functional complexity and regulation in members of Flavobacteria (as
616 determined by 16S rRNA gene; Teeling et al., 2012). From an ecological perspective,
617 these slight functional differences are likely vital to maintain separate niches in the
618 microbial community, ultimately giving each OTU the potential to thrive in changing
619 environmental conditions such as that experienced through an algal bloom rise and
620 decay.

621

622 **Impact of light on organic matter utilization**

623 Free-living bacterial cell and DOC concentrations were significantly lower in the
624 light compared to the dark after incubation with phytodetrital particles. This
625 suggests that either light inhibited bacterial degradation of the particles, which
626 would result in lower bacterial growth and less dissolution of POC into DOC, or light
627 induced more efficient particle degradation due to photoheterotrophic metabolism.
628 In the latter case, labile carbon in the light was either being i) incorporated into
629 larger cells or ii) respired at a higher rate. Since we did not observe any obvious
630 increases in cell size in the light, it seems more plausible that bacteria had, indeed,
631 access to more C in the light and that more of this C was subsequently being
632 respired. Experiments with proteorhodopsin-containing Flavobacteria strains have

633 previously shown that light can enhance the uptake of certain organic molecules (i.e.
634 vitamins, Gómez-Consarnau et al., 2016), which are required for growth, and
635 therefore respiration. Under this scenario, a larger fraction of the organic matter
636 pool would be accessible in the light due to light-enhanced DOM uptake and
637 utilization. However, if we consider photoheterotrophy to be a dominant trait in this
638 microbial community —as a whole— with the potential to increase bacterial fitness,
639 it is puzzling that bacterial abundances were lower in the light incubations. Future
640 research with a higher temporal resolution and more extensive C and N partitioning
641 budgets will be needed to answer this question, and will require quantifying the
642 stable isotopic signal in the particulate, dissolved and gas (i.e. CO_2) fractions during
643 light/dark incubations.

644

645 **Acknowledgements.** Work performed by X. M. and P. K. W. was funded by the U.S.
646 Department of Energy's Office of Biological and Environmental Research Biofuels
647 Science Focus Area Grant SCW1039, and work at LLNL was performed under the
648 auspices of the US Department of Energy at the Lawrence Livermore National
649 Laboratory under Contract DE-AC52-07NA27344. L. G-C. was funded by the Marie
650 Curie Actions–International Outgoing Fellowships (project 253970) and the US
651 National Science Foundation grant OCE1335269.

652
653

References

Alderkamp, A.-C., Van Rijssel, M., and Bolhuis, H. (2007). Characterization of marine bacteria and the activity of their enzyme systems involved in degradation of the algal storage glucan laminarin. *FEMS Microbiol. Ecol.* 59, 108–117. doi:10.1111/j.1574-6941.2006.00219.x.

Allers, E., Gómez-Consarnau, L., Pinhassi, J. H. J., Gasol, J. M., Šimek, K., and Pernthaler, J. (2007). Response of Alteromonadaceae and Rhodobacteriaceae to glucose and phosphorus manipulation in marine mesocosms. *Environ. Microbiol.* 9, 2417–2429. doi:10.1111/j.1462-2920.2007.01360.x.

Azam, F., and Long, R. A. (2001). Oceanography - Sea snow microcosms. *Nature* 414, 495–497. doi:10.1038/35107174.

Beier, S., and Bertilsson, S. (2011). Uncoupling of chitinase activity and uptake of hydrolysis products in freshwater bacterioplankton. *Limnol. Oceanogr.* 56, 1179–1188. doi:10.4319/lo.2011.56.4.1179.

Béjà, O., Aravind, L., Koonin, E. V., Suzuki, M. T., Hadd, A., Nguyen, L. P., et al. (2000). Bacterial rhodopsin: evidence for a new type of phototrophy in the sea. *Science* 289, 1902–1906.

Bidle, K. D., and Azam, F. (1999). Accelerated dissolution of diatom silica by marine bacterial assemblages. *Nature* 397, 508–512.

Bolger, A. M., Lohse, M., and Usadel, B. (2014). Trimmomatic: a flexible trimmer for Illumina sequence data. *Bioinformatics* 30, 2114–2120.

Brindefalk, B., Ekman, M., Ininbergs, K., Dupont, C. L., Yooseph, S., Pinhassi, J. H. J., et al. (2016). Distribution and expression of microbial rhodopsins in the Baltic Sea and adjacent waters. *Environ. Microbiol.* 18, 4442–4455. doi:10.1111/1462-2920.13407.

Brown, M. V., Schwalbach, M. S., Hewson, I., and Fuhrman, J. A. (2005). Coupling 16S-ITS rDNA clone libraries and automated ribosomal intergenic spacer analysis to show marine microbial diversity: development and application to a time series. *Environ. Microbiol.* 7, 1466–1479. doi:10.1111/j.1462-2920.2005.00835.x.

Buchan, A., LeCleir, G. R., Gulvik, C. A., and Gonzalez, J. M. (2014). Master recyclers: features and functions of bacteria associated with phytoplankton blooms. *Nat. Rev. Micro.* 12, 686–698. doi:10.1038/nrmicro3326.

Caporaso J. G., Kuczynski, J., Stombaugh, J., Bittinger, K., Bushman, F. D., Costello, E. K., et al. (2010). *Nature Methods* 7, 335–336. doi:10.1038/nmeth.f.303

Church, M. J., Ducklow, H. W., and Karl, D. M. (2004). Light Dependence of

[3H]Leucine Incorporation in the Oligotrophic North Pacific Ocean. *Appl. Environ. Microbiol.* 70, 4079–4087. doi:10.1128/AEM.70.7.4079-4087.2004.

Dubinsky, V., Haber, M., Burgsdorf, I., Saurav, K., Lehahn, Y., Malik, A., et al. (2017). Metagenomic analysis reveals unusually high incidence of proteorhodopsin genes in the ultraoligotrophic Eastern Mediterranean Sea. *Environ. Microbiol.* 19, 1077–1090. doi:10.1111/1462-2920.13624.

Dumont, M. G., and Murrell, J. C. (2005). Stable isotope probing — linking microbial identity to function. *Nat. Rev. Microbiol.* 3, 499–504. doi: 10.1038/nrmicro1162

Edgar, R. C. (2004). MUSCLE: multiple sequence alignment with high accuracy and high throughput. *Nucleic Acids Res*. 32,1792-1977. doi: 10.1093/nar/gkh340.

Edgar, R. C. (2010). Search and clustering orders of magnitude faster than BLAST. *Bioinformatics* 26, 2460–2461. doi:10.1093/bioinformatics/btq461.

Evans, C., Gómez-Pereira, P. R., Martin, A. P., Scanlan, D. J., and Zubkov, M. V. (2015). Photoheterotrophy of bacterioplankton is ubiquitous in the surface oligotrophic ocean. *Prog. Oceanogr.* 135, 139–145. doi:10.1016/j.pocean.2015.04.014.

Fernández-Gómez, B., Richter, M., Schüler, M., Pinhassi, J. H. J., Acinas, S. G., Gonzalez, J. M., et al. (2013). Ecology of marine Bacteroidetes: a comparative genomics approach. *ISME J.* 7, 1026–1037. doi:10.1038/ismej.2012.169.

Ferrera, I., Gasol, J. M., Sebastian, M., Hojerova, E., and Koblizek, M. (2011). Comparison of Growth Rates of Aerobic Anoxygenic Phototrophic Bacteria and Other Bacterioplankton Groups in Coastal Mediterranean Waters. *Appl. Environ. Microbiol.* 77, 7451–7458. doi:10.1128/AEM.00208-11.

Ferrera, I., Sánchez, O., Kolářová, E., Koblízek, M., and Gasol, J. M. (2017). Light enhances the growth rates of natural populations of aerobic anoxygenic phototrophic bacteria. *ISME J.* 11, 2391–2393. doi:10.1038/ismej.2017.79.

Geng, H., Sale, K. L., Tran-Gyamfi, M. B., Lane, T. W., and Yu, E. T. (2016). Longitudinal Analysis of Microbiota in Microalga Nannochloropsis salina Cultures. *Microb. Ecol.* 72, 14–24. doi:10.1007/s00248-016-0746-4.

Gifford, S. M., Sharma, S., Booth, M., and Moran, M. A. (2013). Expression patterns reveal niche diversification in a marine microbial assemblage. *ISME J.* 7, 281–298. doi:10.1038/ismej.2012.96.

Giovannoni, S. J., Bibbs, L., Cho, J.-C., Stapels, M. D., Desiderio, R. A., Vergin, K. L., et al. (2005). Proteorhodopsin in the ubiquitous marine bacterium SAR11. *Nature* 438, 82–85. doi:10.1038/nature04032.

Gómez-Consarnau, L., Gonzalez, J. M., Coll-Llado, M., Gourdon, P., Pascher, T., Neutze,

R., et al. (2007). Light stimulates growth of proteorhodopsin-containing marine Flavobacteria. *Nature* 445, 210–213. doi:10.1038/nature05381.

Gómez-Consarnau, L., Gonzalez, J. M., Riedel, T., Jaenicke, S., Wagner-Döbler, I., Sañudo-Wilhelmy, S. A., et al. (2016). Proteorhodopsin light-enhanced growth linked to vitamin-B1 acquisition in marine Flavobacteria. *ISME J.* 10, 1102–1112. doi:10.1038/ismej.2015.196.

Gómez-Pereira, P. R., Hartmann, M., Grob, C., Tarran, G. A., Martin, A. P., Fuchs, B. M., et al. (2013). Comparable light stimulation of organic nutrient uptake by SAR11 and Prochlorococcus in the North Atlantic subtropical gyre. *ISME J.* 7, 603–614. doi:10.1038/ismej.2012.126.

Gómez-Pereira, P. R., Schüler, M., Fuchs, B. M., Bennke, C., Teeling, H., Waldmann, J., et al. (2012). Genomic content of uncultured Bacteroidetes from contrasting oceanic provinces in the North Atlantic Ocean. *Environ. Microbiol.* 14, 52–66. doi:10.1111/j.1462-2920.2011.02555.x.

Gonzalez, J. M., Fernandez-Gomez, B., Fernandez-Guerra, A., Gómez-Consarnau, L., Sanchez, O., Coll-Llado, M., et al. (2008). From the Cover: Genome analysis of the proteorhodopsin-containing marine bacterium Polaribacter sp. MED152 (Flavobacteria). *Proc. Natl. Acad. Sci. U.S.A.* 105, 8724–8729. doi:10.1073/pnas.0712027105.

Grossart, H.-P., Tang, K. W., Kiørboe, T., and Ploug, H. (2007). Comparison of cell-specific activity between free-living and attached bacteria using isolates and natural assemblages. *FEMS Microbiol. Lett.* 266, 194–200. doi:10.1111/j.1574-6968.2006.00520.x.

Guillard RRL (1975) Culture of phytoplankton for feeding marine invertebrates. In: Smith WL, Chanley MH (eds) Culture of marine invertebrate animals. Plenum Press, New York, p 26-60

Guillou, L., Bachar, D., Audic, S., Bass, D., Berney, C., Bittner, L. (2013). The Protist Ribosomal Reference database (PR^2): a catalog of unicellular eukaryote Small Sub-Unit rRNA sequences with curated taxonomy. *Nucleic Acids Res*. 41, D597–D604. doi: 10.1093/nar/gks1160

Guindon, S., Dufayard, J.F., Lefort, V., Anisimova, M., Hordijk, W., Gascuel, O. (2010). New Algorithms and Methods to Estimate Maximum-Likelihood Phylogenies: Assessing the Performance of PhyML 3.0. *Syst. Biol.* 59:307-321.

Hagström, A., Azam, F., Berg, C., and Zweifel, U. L. (2018). Isolates as models to study bacterial ecophysiology and biogeochemistry. *Aquat. Microb. Ecol.* 80, 15–27. doi:10.3354/ame01838.

Hobbie, J. E., Daley, R. J., and Jasper, S. (1977). Use of nuclepore filters for counting

bacteria by fluorescence microscopy. *Appl. Environ. Microbiol.* 33, 1225–1228.

Inoue, K., Ono, H., Abe-Yoshizumi, R., Yoshizawa, S., Ito, H., Kogure, K., et al. (2013). A light-driven sodium ion pump in marine bacteria. *Nat. Comms.* 4, 1678. doi:10.1038/ncomms2689.

Kiorboe, T., Tang, K., Grossart, H.-P., and Ploug, H. (2003). Dynamics of microbial communities on marine snow aggregates: Colonization, growth, detachment, and grazing mortality of attached bacteria. *Appl. Environ. Microbiol.* 69, 3036–3047. doi:10.1128/AEM.69.6.3036-3047.2003.

Kirchman, D. L. (2002). The ecology of Cytophaga-Flavobacteria in aquatic environments. *FEMS Microbiol. Ecol.* 39, 91–100. doi:10.1111/j.1574-6941.2002.tb00910.x.

Koblížek, M. (2015). Ecology of aerobic anoxygenic phototrophs in aquatic environments. *FEMS Microbiol. Rev.* 39, 854-70. doi: 10.1093/femsre/fuv032

Kolber, Z. S., Van Dover, C. L., and Falkowski, P. G. (2000). Bacterial photosynthesis in surface waters of the open ocean. *Nature* 407, 177-179.

Love, M. I., Huber, W., and Anders, S. (2014). Moderated estimation of fold change and dispersion for RNA-seq data with DESeq2. *Genome Biol.* 15. doi:10.1186/s13059-014-0550-8.

Ludwig, W., Strunk, O., Westram, R., Richter, L., Meier, H., Yadhukumar, et al. (2004). ARB: a software environment for sequence data. *Nucleic Acids Res.* 32, 1363–1371. doi:10.1093/nar/gkh293.

Maresca, J. A., Miller, K. J., Keffer, J. L., Sabanayagam, C. R., and Campbell, B. J. (2018). Distribution and Diversity of Rhodopsin-Producing Microbes in the Chesapeake Bay. *Appl. Environ. Microbiol.* 84, e00137–18.

Martin, M. (2011). Cutadapt removes adapter sequences from high-throughput sequencing reads. *EMBnet.journal*, 17, 10-12. doi:https://doi.org/10.14806/ej.17.1.200.

Mary, I., Tarran, G. A., Warwick, P. E., Terry, M. J., Scanlan, D. J., Burkill, P. H., et al. (2008). Light enhanced amino acid uptake by dominant bacterioplankton groups in surface waters of the Atlantic Ocean. *FEMS Microbiol Ecol*. 63,36-45. doi: 10.1111/j.1574-6941.2007.00414.x

Mayali, X., Stewart, B., Mabery, S., and Weber, P. K. (2016). Temporal succession in carbon incorporation from macromolecules by particle-attached bacteria in marine microcosms. *Environ. Microbiol. Rep.* 8, 68–75. doi:10.1111/1758-2229.12352.

Mayali, X., Weber, P. K., Brodie, E. L., Mabery, S., Hoeprich, P. D., and Pett-Ridge, J. (2012). High-throughput isotopic analysis of RNA microarrays to quantify microbial resource use. *ISME J.* 6, 1210–1221. doi:10.1038/ismej.2011.175.

Mayer, L. M., Schick, L.L., Hardy, K. R., Estapa, M. L. (2009). Photodissolution and other photochemical changes upon irradiation of algal detritus. *Limnol. Oceanogr.* 54, 1688–1698

McMurdie, P. J., and Holmes, S. (2013). phyloseq: An R Package for Reproducible Interactive Analysis and Graphics of Microbiome Census Data. *PLoS ONE* 8. doi:10.1371/journal.pone.0061217.

Michelou, V. K., Cottrell, M. T., and Kirchman, D. L. (2007). Light-Stimulated Bacterial Production and Amino Acid Assimilation by Cyanobacteria and Other Microbes in the North Atlantic Ocean. *Appl. Environ. Microbiol.* 73, 5539–5546. doi:10.1128/AEM.00212-07.

Milledge, J. J., and Heaven, S. (2013). A review of the harvesting of micro-algae for biofuel production. *Rev. Environ. Sci. Bio*. 12, 165–178. doi:10.1007/s11157-012-9301-z.

Morris, J. J., Lenski, R. E., Zinser, E. R. (2012). The black queen hypothesis: evolution of dependencies through adaptive gene loss. mBio 3:e00036 -12. https://doi.org/10.1128/mBio.00036-12.

Needham, D. M., Chow, C. E. T., Cram, J. A., Sachdeva, R., Parada, A., & Fuhrman, J. A. (2013). Short-term observations of marine bacterial and viral communities: patterns, connections and resilience. *ISME J*. 7:1274-1285. doi: 10.1038/ismej.2013.19

Needham, D. M., Fuhrman, J. A. (2016). Pronounced daily succession of phytoplankton, archaea and bacteria following a spring bloom. *Nature Microbiol.* DOI: 10.1038/NMICROBIOL.2016.5

Needham, D. M., Fichot, E. B., Wang, E., Berdjeb, L., Cram, J. A., Fichot, C. G., Fuhrman, J. A. (2018). Dynamics and interactions of highly resolved marine plankton via automated high-frequency sampling. *ISME J.* 12, 2417-2432. doi:10.1038/s41396-018-0169-y.

Ottesen, E. A., Young, C. R., Eppley, J. M., Ryan, J. P., Chavez, F. P., Scholin, C. A., et al. (2013). Pattern and synchrony of gene expression among sympatric marine microbial populations. *Proc. Natl. Acad. Sci. U.S.A.* 110, E488–497. doi:10.1073/pnas.1222099110.

Ottesen, E. A., Young, C. R., Gifford, S. M., Eppley, J. M., and Marin, R. (2014). Multispecies diel transcriptional oscillations in open ocean heterotrophic bacterial assemblages. *Science* 345, 204-207. doi:10.1126/science.1252717.

Parada, A. E., Needham, D. M., and Fuhrman, J. A. (2016). Every base matters: assessing small subunit rRNA primers for marine microbiomes with mock communities, time series and global field samples. *Environ. Microbiol.* 18, 1403–1414. doi:10.1111/1462-2920.13023.

Passow, U., Engel, A., and Ploug, H. (2003). The role of aggregation for the dissolution of diatom frustules. *FEMS Microbiol. Ecol.* 46, 247–255. doi:10.1016/S0168-6496(03)00199-5.

Pinhassi, J. H. J., DeLong, E. F., Beja, O., Gonzalez, J. M., and Pedrós-Alió, C. (2016). Marine Bacterial and Archaeal Ion-Pumping Rhodopsins: Genetic Diversity, Physiology, and Ecology. *Microbiol. Mol. Biol. Rev.* 80, 929–954. doi:10.1128/MMBR.00003-16.

Ploug, H. (2001). Small-scale oxygen fluxes and remineralization in sinking aggregates. *Limnol. Oceanogr.* 46, 1624–1631.

Pruesse, E., Quast, C., Knittel, K., Fuchs, B. M., Ludwig, W., Peplies, J., et al. (2007). SILVA: a comprehensive online resource for quality checked and aligned ribosomal RNA sequence data compatible with ARB. *Nucleic Acids Res.* 35, 7188–7196. doi:10.1093/nar/gkm864.

Quast, C., Pruesse, E., Yilmaz, P., Gerken, J., Schweer, T., Yarza, P., et al. (2013). The SILVA ribosomal RNA gene database project: improved data processing and web-based tools. *Nucleic Acids Res*. 41, D590–D596. doi: 10.1093/nar/gks1219

Riedel, T., Gómez-Consarnau, L., Tomasch, J., Martin, M., Jarek, M., Gonzalez, J. M., et al. (2013). Genomics and Physiology of a Marine Flavobacterium Encoding a Proteorhodopsin and a Xanthorhodopsin-Like Protein. *PLoS ONE* 8, e57487. doi:10.1371/journal.pone.0057487.s007.

Rontani J-F. (2001) Visible light-dependent degradation of lipidic phytoplanktonic components during senescence: a review. *Photochemistry*. 58, 187-202.

Ruiz-González, C., Simó, R., Sommaruga, R., Gasol, J. M. (2013). Away from darkness: a review on the effects of solar radiation on heterotrophic bacterioplankton activity. *Front Microbiol*. 4, 131. doi: 10.3389/fmicb.2013.00131.

Sarmento, H., and Gasol, J. M. (2012). Use of phytoplankton-derived dissolved organic carbon by different types of bacterioplankton. *Environ. Microbiol.* 14, 2348–2360. doi:10.1111/j.1462-2920.2012.02787.x.

Shanks, A. L., and Edmodson, E. W. (1989). Laboratory-Made Artificial Marine Snow - a Biological Model of the Real Thing. *Mar. Biol.* 101, 463–470.

Sieradzki, E. T., Fuhrman, J. A., Rivero-Calle, S., and Gomez-Consarnau, L. (2018). Proteorhodopsins dominate the expression of phototrophic mechanisms in

seasonal and dynamic marine picoplankton communities. *PeerJ* 6, e5798. doi:10.7717/peerj.5798.

Simon, M., Grossart, H.-P., Schweitzer, B., and Ploug, H. (2002). Microbial ecology of organic aggregates in aquatic ecosystems. *Aquat. Microb. Ecol.* 28, 175–211.

Singh-Gasson, S., Green, R. D., Yue, Y., Nelson, C., Blattner, F., Sussman, M. R., et al. (1999). Maskless fabrication of light-directed oligonucleotide microarrays using a digital micromirror array. *Nat Biotechnol.* 17, 974-978. doi: 10.1038/13664

Teeling, H., Fuchs, B. M., Becher, D., Klockow, C., Gardebrecht, A., Bennke, C. M., et al. (2012). Substrate-Controlled Succession of Marine Bacterioplankton Populations Induced by a Phytoplankton Bloom. *Science* 336, 608–611. doi:10.1126/science.1218344.

Teeling, H., Fuchs, B. M., Bennke, C. M., Krueger, K., Chafee, M., Kappelmann, L., et al. (2016). Recurring patterns in bacterioplankton dynamics during coastal spring algae blooms. *Elife* 5. doi:10.7554/eLife.11888.

Unanue, M., Azúa, I., Arrieta, J., Labirua-Iturburu, A., Egea, L., and Iriberri, J. (1998). Bacterial Colonization and Ectoenzymatic Activity in Phytoplankton-Derived Model Particles: Cleavage of Peptides and Uptake of Amino Acids. *Microb. Ecol.* 35, 136–146.

Wang, Q., Garrity, G. M., Tiedje, J. M., Cole, J. R. (2007). Naive Bayesian classifier for rapid assignment of rRNA sequences into the new bacterial taxonomy. *Appl Environ Microbiol.* 73, 5261-6267.

Wagner-Döbler, I., and Biebl, H. (2006). Environmental Biology of the Marine RoseobacterLineage. *Annu. Rev. Microbiol.* 60, 255–280. doi:10.1146/annurev.micro.60.080805.142115.

Williams, T. J., Wilkins, D., Long, E., Evans, F., DeMaere, M. Z., Raftery, M. J., et al. (2013). The role of planktonic Flavobacteria in processing algal organic matter in coastal East Antarctica revealed using metagenomics and metaproteomics. *Environ. Microbiol.* 15, 1302–1317. doi:10.1111/1462-2920.12017.

Wright, E. S., Yilmaz, L. S., and Noguera, D. R. (2012). DECIPHER, a search-based approach to chimera identification for 16S rRNA sequences. *Appl. Environ. Microbiol.* 78, 717–725. doi:10.1128/AEM.06516-11.

Yoshizawa, S., Kumagai, Y., Kim, H., Ogura, Y., Hayashi, T., Iwasaki, W., et al. (2014). Functional characterization of flavobacteria rhodopsins reveals a unique class of light-driven chloride pump in bacteria. *Proc. Natl. Acad. Sci. U.S.A.* doi:10.1073/pnas.1403051111.

Figure legends

Figure 1. Bacterial cell abundances and dissolved organic carbon (DOC) concentrations in the control and particle addition treatments after a 72 hour incubation, showing increased DOC and bacterial concentrations in the particle incubations compared to the no-addition controls, as well as a statistically significant positive correlation between the two variables. This pattern applied to both the incubations with particles and the controls, regardless of being exposed to continuous light or darkness.

Figure 2. Microbial community structure identified down to the order level after 72-hour incubations in light or darkness, in the particle attached (>5 μm) and free-living (5 to 0.2 μm) fractions, and controls (no particle addition) obtained from 16S rRNA gene sequencing. Numbers refer to read percentages affiliated with the particular taxa.

Figure 3. Heatmaps of OTUs that had significant shifts between the various experimental treatments. **(A)** OTUs are ordered by their phylogenetic relatedness of the partial 16S amplicon sequence as shown in the tree to the left, where the OTUs from the current study are in black text, reference genome sequences are in red, and OTUs from a natural phytoplankton bloom at the San Pedro Ocean Time-series location are in blue. For OTUs from the current study, they are annotated with treatments (Light or Dark, Large or Small) in which they were significant higher ($p < 0.05$) following the taxon name, where "Light", and "Dark", "Small", "Large", corresponds to light incubation, dark incubation, smaller size fraction (0.2 - 5 μm), or larger size fraction (>5 μm), respectively. "NA" indicates that an OTU was not significantly higher in either of the respective treatments. Relative abundances of OTUs are scaled by both their **(B)** z-scores and **(C)** relative read proportions with no transformation. Only OTUs that had relative abundances of greater than 0.25% in any of the experimental treatments are shown.

Figure 4. Family-level contribution of ^{15}N incorporation from diatom-derived particles in the two treatments and size fractions. Calculations are based on taxon-specific isotope incorporation (HCE, measured by Chip-SIP) multiplied by their relative abundances based on 16S rRNA gene sequencing.

Figure 1

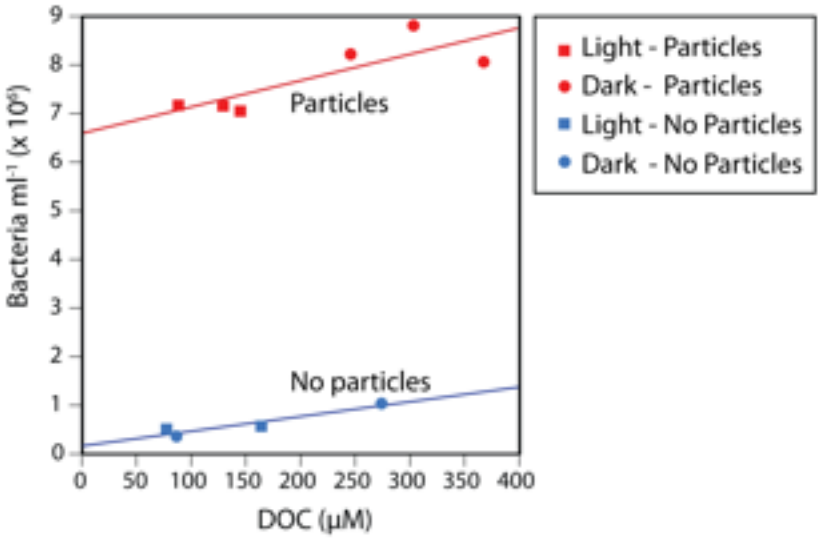
Bacteria ml^{-1} (x 10^6)
DOC (µM)
Particles
No particles
Light - Particles
Dark - Particles
Light - No Particles
Dark - No Particles

Figure 2

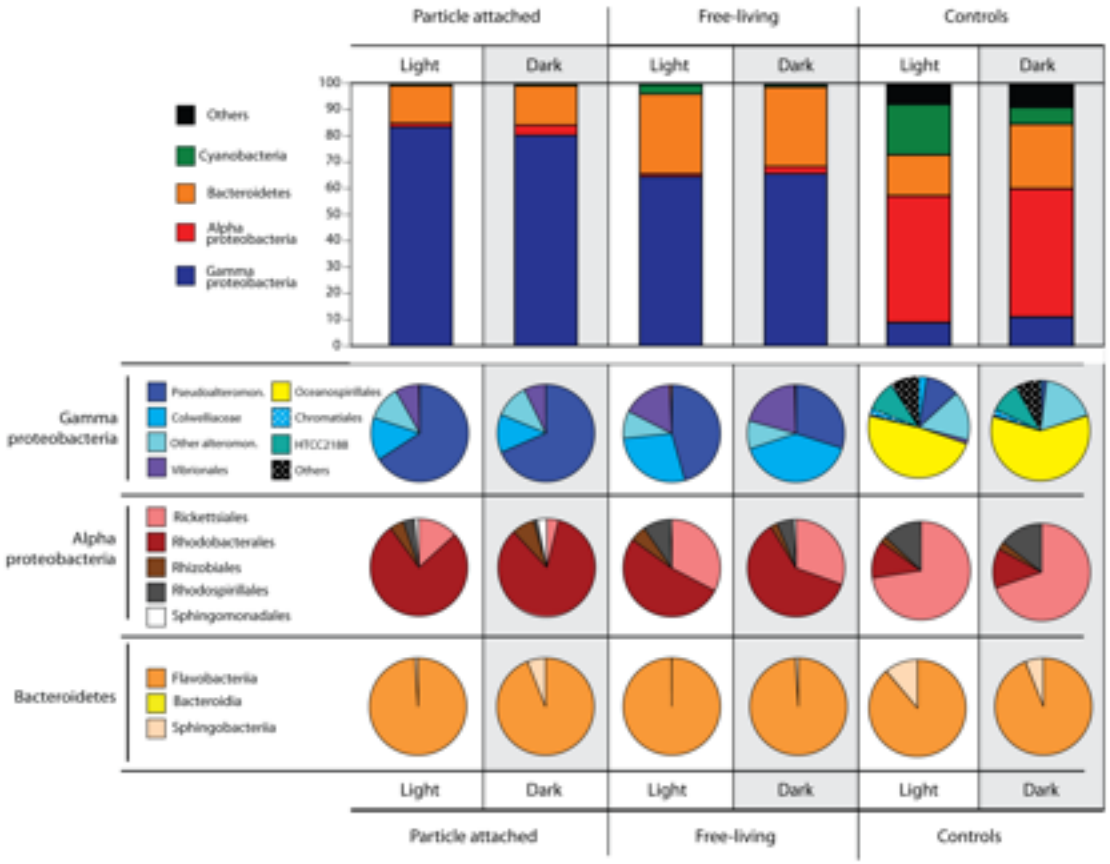
Particle attached
Free-living
Controls
Light
Dark
Others
Cyanobacteria
Bacteroidetes
Alpha proteobacteria
Gamma proteobacteria
100
90
80
70
60
50
40
30
20
10
0
Gamma proteobacteria
Pseudoalteromon.
Colwelliaceae
Other alteromon.
Vibrionales
Oceanospirillales
Chromatiales
HTCC2188
Others
Alpha proteobacteria
Rickettsiales
Rhodobacterales
Rhizobiales
Rhodospirillales
Sphingomonadales
Bacteroidetes
Flavobacteriia
Bacteroidia
Sphingobacteriia

Figure 3

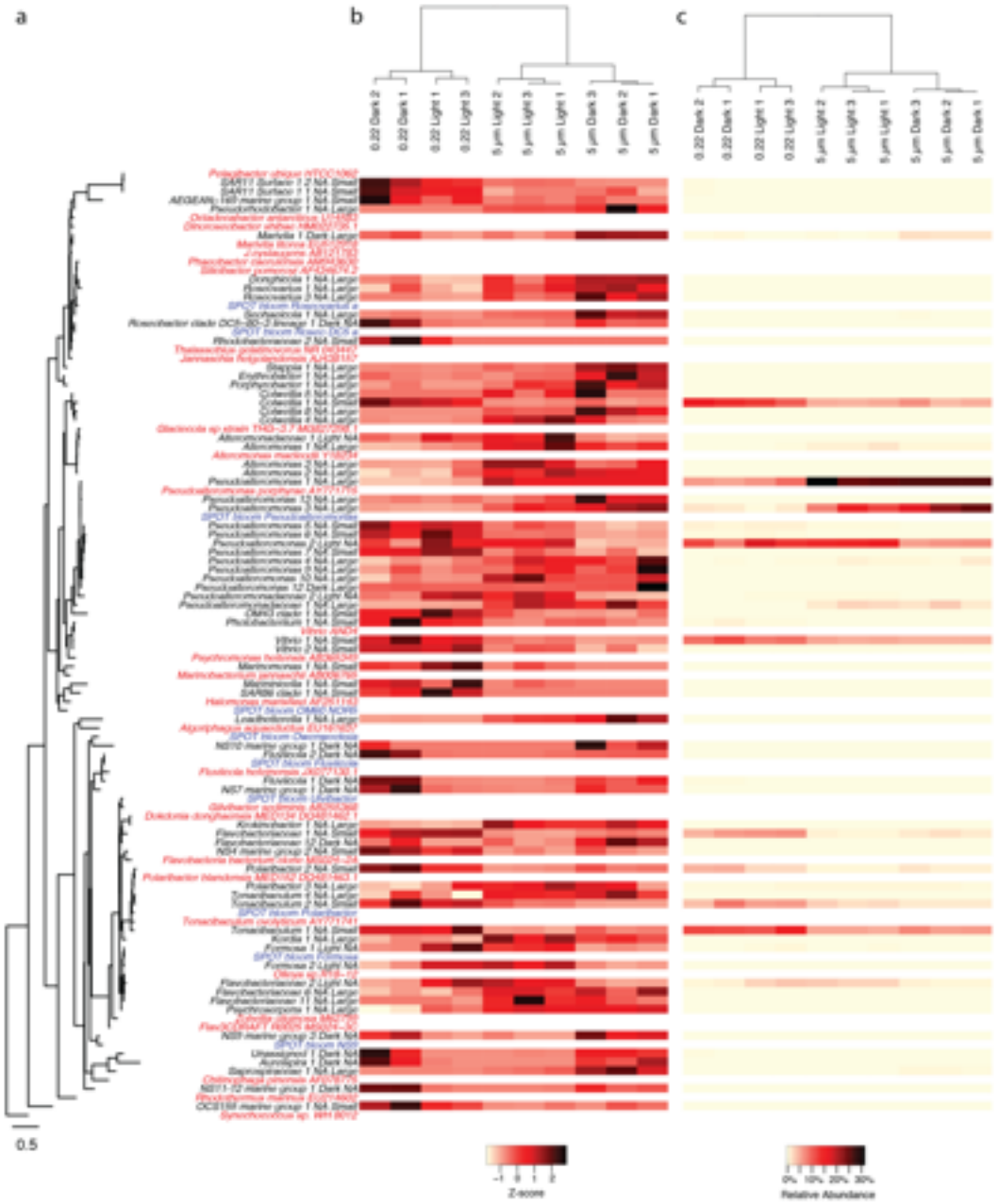
a
b
c
0.22 Dark 2
0.22 Dark 1
0.22 Light 1
0.22 Light 3
5 µm Light 2
5 µm Light 3
5 µm Light 1
5 µm Dark 3
5 µm Dark 2
5 µm Dark 1
0.5
Z-score
Relative Abundance

Figure 4

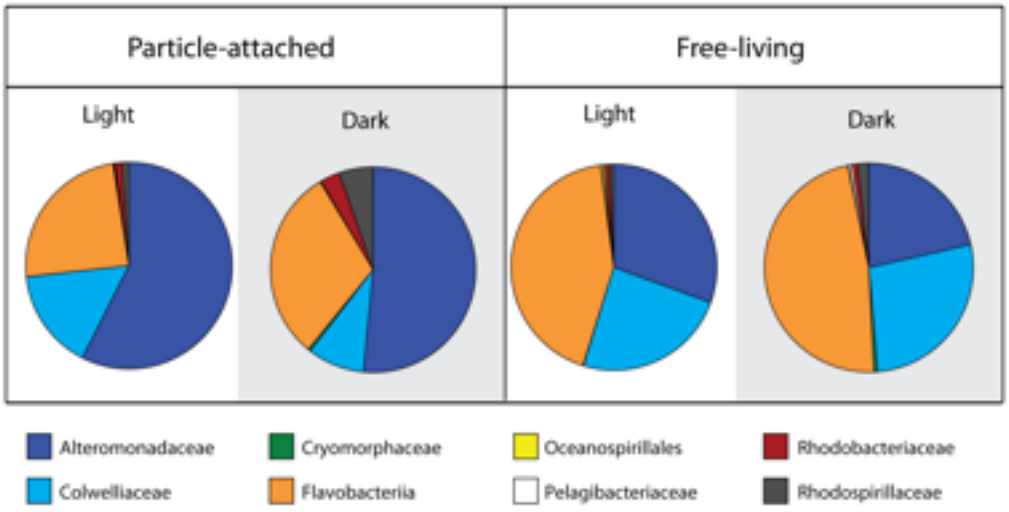
Particle-attached
Free-living
Light
Dark
Light
Dark
Alteromonadaceae
Colwelliaceae
Cryomorphaceae
Flavobacteriia
Oceanospirillales
Pelagibacteriaceae
Rhodobacteriaceae
Rhodospirillaceae

Table 1. Summary of covariance analysis (ANCOVA) results showing OTUs with statistically significant treatment differences for incorporation of ^{15}N from particles. Several examples are shown in more detail in Figure S4.

			Particle attached		Free-living	light	Dark
OTU	Taxonomy	GB accession	higher in light	higher in dark	higher in light	Higher in free-living	Higher in free-living
Owenweeksia_B	Bacteria;Bacteroidetes;Flavobacteria_Flavobacteriales;Cryomorphaceae_Owenweeksia	KC287128	X		X		X
Colwellia_1A	Bacteria;Gammaproteobacteria;Alteromonadales_1;Colwelliaceae;Colwellia_1	KC287092	X			X	X
Pseudoalteromonas_A	Bacteria;Gammaproteobacteria;Alteromonadales_1;Pseudoalteromonas	KC287096	X				X
Maribacter	Bacteria;Bacteroidetes;Flavobacteria_Flavobacteriales;Flavobacteriaceae_1;Maribacter	KC287125	X				X
Colwellia_1B	Bacteria;Gammaproteobacteria;Alteromonadales_1;Colwelliaceae;Colwellia_1	KC287093	X				X
Flavobacterium_1B	Bacteria;Bacteroidetes;Flavobacteria_Flavobacteriales;Flavobacteriaceae_1;	KC287124	X				
890_1_C_2	Bacteria;BD1-5	KF227631		X		X	X
890_1_E_8	Bacteria;Gammaproteobacteria;Legionellales;Legionellaceae;uncultured	JF767288		X		X	
SPOTSMAY03_890m27	Bacteria;Gammaproteobacteria;Oceanospirillales;Oceanospirillaceae;Pseudospirillum	DQ009470		X			
SPOTSAPR01_5m177	Bacteria;Gammaproteobacteria;Oceanospirillales;OM182 clade	DQ009128		X			
890_2_B_8	Bacteria;Actinobacteria;Acidimicrobiia;Acidimicrobiales;Sva0996 marine group	KF227626		X			
890_1_G_6	Bacteria;Bacteroidetes;Flavobacteria;Flavobacteriales;Flavobacteriaceae;uncultured	KY282445		X			
890_1_G_2	Bacteria;Alphaproteobacteria;Rhodospirillales;Rhodospirillaceae;uncultured	KF227741		X			
SPOTSMAY03_890m21	Bacteria;Gammaproteobacteria;Alteromonadales;Alteromonadaceae;SAR92 clade	DQ009469				X	X
SPOTSAUG01_5m75	Bacteria;Gammaproteobacteria;Thiotrichales;Piscirickettsiaceae;uncultured	DQ009136				X	X
Oceanobacter_A	Bacteria;Gammaproteobacteria;Oceanospirillales_Oceanospirillaceae_2;Oceanobacter	KC287100				X	X
Maritalea	Bacteria;Alphaproteobacteria;Rhizobiales_1;Hyphomicrobiaceae;Maritalea	KC287120				X	X
Glaciecola_1	Bacteria;Gammaproteobacteria;Alteromonadales_1;Alteromonadaceae_1;Glaciecola	KC287090				X	X
Clostridium	Bacteria;Firmicutes;Clostridia_1;Clostridiales;Ruminococcaceae;uncultured	KC287133				X	X
Alcanivora_AB	Bacteria;Gammaproteobacteria;Oceanospirillales_Alcanivoraceae_Alcanivora	KC287107				X	X
890_2_F_10	Bacteria;Proteobacteria;CF2	KF227740				X	X
SPOTSAPR01_5m148	Bacteria;Deferribacteres;Deferribacteres;Deferribacterales;SAR406 clade (Marine group A)	DQ009148				X	
SPOTSAPR01_5m105	Bacteria;Alphaproteobacteria;Rhodobacterales_Rhodobacteriaceae_1;uncultured	DQ009158				X	
890_4_D_5	Bacteria;Lentisphaerae;Lentisphaeria;Lentisphaerales;Lentisphaeraceae;Lentisphaera	AB703829				X	
890_4_B_7	Bacteria;Bacteroidetes;Flavobacteria;Flavobacteriales;NS9 marine group	KF227727				X	
Roseobacter_B	Bacteria;Alphaproteobacteria;Rhodobacterales_Rhodobacteriaceae_1;uncultured	KC287113					X
Oceaniserpentilla	Bacteria;Gammaproteobacteria;Oceanospirillales_Oceanospirillaceae_2;Oceaniserpentilla	KC287102					X
JTB148	Bacteria;Gammaproteobacteria;JTB148	KC287110					X
Hyphomonas	Bacteria;Alphaproteobacteria;Caulobacter_Hyphomonadaceae;Hyphomonas;Hyphomonas_1	KC287118					X
Colwellia_2	Bacteria;Gammaproteobacteria;Alteromonadales_1;Colwelliaceae;Colwellia_2	KC287094					X
890_2_G_5	Bacteria;Alphaproteobacteria;Rhodospirillales;Rhodospirillaceae;Defluviicoccus	KF227655					X